

# Statistical and Dynamical Study of Disease Propagation in a Small World Network

Nouredine Zekri<sup>1,2\*</sup> and Jean Pierre Clerc<sup>1†</sup>

<sup>1</sup>I.U.S.T.I., Technopôle Château Gombert, Université de Provence, Marseille, France.

<sup>2</sup>U.S.T.O., Département de Physique, L.E.P.M., B.P.1505 El M'Naouar, Oran, Algérie.

January 14, 2022

## Abstract

We study numerically statistical properties and dynamical disease propagation using a percolation model on a one dimensional small world network. The parameters chosen correspond to a realistic network of school age children. We found that percolation threshold decreases as a power law as the short cut fluctuations increase. We found also the number of infected sites grows exponentially with time and its rate depends logarithmically on the density of susceptibles. This behavior provides an interesting way to estimate the serology for a given population from the measurement of the disease growing rate during an epidemic phase. We have also examined the case in which the infection probability of nearest neighbors is different from that of short cuts. We found a double diffusion behavior with a slower diffusion between the characteristic times.

**Keywords:** Small world, percolation, epidemics.

PACS Number(s): 87.23.Ge, 05.40.-a, 05.70.Jk, 64.60.Fr

---

\*Email zekri@mail.univ-usto.dz

†Email clair@iusti.univ-mrs.fr

# 1 Introduction

To model disease propagation, it is necessary to define the corresponding social network connecting any two individuals in the world. The expected properties of such a network should be both the clustering (which excludes models of disorder like the random graphs [1]), and to allow a connection between any two individuals within a finite number of steps (which excludes the regular networks with only nearest neighbor connections). Indeed, for the latter feature Milgram showed in 1967 that the average number of steps connecting any two individuals is six (called also six degrees of separation) [2]. This behavior led recently Watts and Strogatz to propose the model of Small World Network (*SWN*) [3, 4]. They considered a low dimensional network with periodic boundary conditions for convenience (a ring for example) where they rewired some bonds with a probability  $\phi$  to a new site randomly chosen from the network. For small values of  $\phi$  this still corresponds to a regular network but with few long range connections called Short-Cuts (*SC*). A more recent work on the *SWN* was proposed by Newman and Watts [5] where the number  $k$  of Nearest Neighbors (*NN*) is conserved but instead of rewiring, they added an average density  $\phi$  of new bonds from each site  $i$  to other nodes randomly chosen (except its nearest neighbors). A review of these models and their application to various fields and particularly epidemics can be found in the references [3, 6]. In these networks the percolation threshold was extensively investigated and its dependence to the *NN* and *SC* was found to satisfy the following equation [5, 7]

$$\phi = \frac{(1 - p_c)^{k/2}}{p_c} \quad (1)$$

This threshold corresponds in epidemics to the smallest concentration of susceptibles leading to the outbreak [5]. However, the statistical behavior of percolative *SWN* networks is different from that of regular systems [8]. In particular, at the percolation threshold, there is no diverging cluster for the *SWN* because a *SC* between the two ends of the system has a finite probability to occur for any non-vanishing number of these bonds. On the other hand, the characteristic length scale in such networks (which corresponds to the correlation length in regular lattices) behaves as  $\phi^{-1/d}$ ,  $d$  being the euclidean dimension of the system [7]. It is then obvious that this characteristic length

does not diverge at the percolation threshold for such networks. Therefore, a further investigation of the cluster statistics around this *new* percolation threshold for such networks and the phase transition seems to be necessary.

Let us now consider the application of this model to epidemics which seems to be one of its main aims. From the large amount of works using *SWN*, there is no direct comparison with the existing data may be due to the complexity of the diseases features (incubation and latent periods, birth and death rates etc.). Furthermore, the parameters used (mainly  $\phi$ ) are very small and do not simulate the real connections between individuals. They use also commonly average values of the *NN* and the *SC* while these quantities strongly fluctuate in the real live (the number of contacts, friends, family members etc. varies from 0 to few tens) which can influence sensitively the results on the density of susceptibles at the percolation threshold (epidemic outbreak). On the other hand, it is impossible in practice to measure the density of susceptibles systematically (it needs an extensive serological investigation in the epidemic phase). Generally, for large population samples epidemiologists measure the evolution with time of the number of cases for a given disease. It is then necessary to study the dynamical behavior of the propagation of the disease and relate it to the density of susceptibles. There are only few works which examined (only qualitatively) the dynamical behavior of the disease on social networks [9, 10, 11]. The aim of these works was to show how the density of infected behaves in the endemic and epidemic phases.

In this article, we use a site percolation on a *SWN* with parameters ( $k$  and  $\phi$ ) representing a sample of school age children to study the effect of the fluctuations of *NN* and *SC* on the percolation threshold. Furthermore, in order to propose a formula for determining the serology of the sample from the rate of increase of the number of cases, we investigate also extensively the dynamical behavior of an infectious disease as well as its effect on the density of susceptibles below and above the percolation threshold. A new *super-diffusion* is found above the percolation threshold when the cluster is initially infected by one or a small number of infectious sites and its characteristic time dependence on the density of susceptibles is determined. We examined also the case where the infection probability of the *NN* is different from that of *SC*, showing a

double diffusion with two characteristic times. In the next section we describe the model and then present the results on the statistics of the clusters and the percolation threshold. The results on the dynamical behavior of the disease are presented in section 4.

## 2 Model description

We consider the one dimensional *SWN* described by Newman and Watts [5] but  $\phi$  represents the total number of *SC* generated for each site uniformly from all the other sites of the network. In the case where  $k$  and  $\phi$  are not fixed they are generated randomly within a normal distribution centered at their average values with fluctuations  $\delta k$  and  $\delta\phi$  respectively. The coordination number is the total number of bonds to a given site ( $z = k + \phi$ ). We study in this network a site percolation problem [8] by assuming each susceptible site  $j$  (occupied) contracts the disease if it is connected with an ill site  $i$  (occupied also). The occupied sites (susceptibles) are randomly generated with a concentration  $p$  while the empty sites correspond to refracted individuals. For  $k$  and  $\phi$  fixed, the percolation threshold  $p_c$  is related to  $k$  and  $\phi$  by Eq.(1) [7]. This threshold corresponds to a transition from the endemic phase below  $p_c$  to the epidemic one above this point [10]. In *SWN* networks,  $p_c$  is the minimum concentration of occupied sites above which the average largest cluster size  $\xi$  of the occupied sites becomes power-law increasing with the concentration ( $\xi = (p - p_c)^x$ ), while it diverges in a regular network [8] (note here that the exponent  $x$  is positive). By analogy with the regular lattices [8], we will check the universality of the exponent  $x$ .

We are interested in the application of such a model to a childhood disease like measles. In such diseases epidemiological investigations on school age children can be easily controlled and provide data with a minimum bias. We choose parameter values corresponding to such a disease by taking  $k = 2$  to be the average number of brothers, sisters and neighbors, while  $\phi = 30$  represents the average number of children one can meet at the school. These parameters should correspond to a topology closer to that encountered in a real social network. Regarding the dynamical study, we assume the major contribution to the epidemics provided by the largest cluster. We restrict ourselves then to this cluster and start the infection with one or few infectious sites at time 0.

These sites will infect all the connected sites in the next step (after a time  $\Delta t$ ), which themselves infect their connected sites after  $2\Delta t$  and so on. We assume the latent and incubation periods smaller than  $\Delta t$  which is taken in the rest of this paper as a unit time. The number of infected sites in each step is averaged by varying the initial infectious site position through the whole cluster.

### 3 Percolation threshold and cluster distribution

In this section, we realize 100 configurations of the network described in the previous section with a size fixed at 100000 sites. We examine the effects of  $\phi$  and its fluctuations on the average cluster sizes,  $p_c$  and  $x$ . Finally, we investigate the cluster size distribution around  $p_c$  in order to determine the main contribution to the propagation of the disease.

In figure 1a we show the variation of the cluster size with the concentration of occupied sites for three different cases:  $\phi = 6, 30$  (fixed values) and for  $k$  and  $\phi$  randomly generated with a normal distribution centered at 2 and 30 respectively, with a fluctuation of 2 et 15 respectively. We see clearly from this figure that in all cases the cluster sizes vary as a power law of  $(p - p_c)$  above  $p_c$ . For fixed  $k$  and  $\phi$  the value of  $p_c$  is in a good agreement with the analytical predictions of Newman et al. [7] (Eq. 1). However, in the case of fluctuations of  $k$  and  $\phi$ , this threshold decreases sensitively (about 50% in the case shown in Fig.1a) as the fluctuations increase. Therefore, the average values of  $k$  and  $\phi$  are not sufficient to characterize an epidemic outbreak. The  $SC$  fluctuations  $\delta\phi$  decrease  $p_c$  as a power law with an exponent 0.1 (as shown in figure 1b), indicating a sensitive participation of the larger values of  $\phi$  to built the largest cluster. Therefore, the percolation threshold behaves as

$$p_c \simeq \phi^{-1} \delta\phi^{-0.1} \quad (2)$$

From this behavior, we can estimate the percolation threshold in a real sample of school age children to be in the range 2.3% to 2.8%.

Now let us restrict ourselves to the case of fixed  $k = 2$  and  $\phi = 6$  in order to examine the statistical behavior of the clusters around  $p_c$  (without loss of generality, these values are chosen

only because  $p_c$  is large enough to enable sufficient cluster statistics for such a sample size) . We found that the cluster size fluctuations are maximum at this threshold (see Fig.2a) implying a divergence of this quantity at  $p_c$  which seems to be a signature of a phase transition. The cluster size distribution (see figure 2b) confirms this divergence since it decreases exponentially below  $p_c$  while it is power-law decreasing at this threshold (this power law behavior is in agreement with the results of Castellano et al. [12] on other systems). Indeed, at  $p_c$  this corresponds to a Lévy distribution [13] with an exponent of 2.13 indicating the divergence of all its moments. We notice here that only the higher sizes (rare events) contribute to the outbreak at  $p_c$  (as expected in such distributions). Above  $p_c$  the small size clusters are *absorbed* by the largest one and we have again an exponentially decreasing distribution for small clusters while there is only one very large cluster (not shown in Fig.2b).

Since the cluster size does not diverge at  $p_c$ , it is obvious that  $x$  is not universal (because it is not a critical exponent), but it is interesting to know how it depends on  $\phi$  in such lattices. In figure 2c, the exponent  $x$  seems to vary only linearly for larger values of  $\phi$  but with a very small slope (about  $5.6 \cdot 10^{-3}$ ). It is difficult to predict its behavior for very small values of  $\phi$  because in this case the network tends to a regular one and the cluster size becomes very large so that the sample sizes taken here do not allow us to measure this exponent accurately.

However, even if the parameters chosen in this model are close to those of a real social network, it seems impossible for epidemiologists to check these results. Indeed, as explained below, they cannot measure the density of susceptibles, except if they investigate systematically the serology of a sufficiently large sample of school age children (e.,e.g. for a city sample). Therefore, the behavior of  $p_c$  should be checked for measurable quantities. In the case of disease propagation, the time dependence of the number of cases can be directly measured by epidemiological techniques. We will investigate this dynamical behavior in the following section.

## 4 Dynamical study of the propagation of a disease

In this section we restrict ourselves to the fixed values of  $k$  and  $\phi$  (2 and 30 respectively) to simulate a sample of school age children. From the results of Fig.2b, we assume that the main growing effect of the infection comes from the largest cluster and estimate the propagation time of the epidemics only from this cluster. We determine the evolution with time of the number of cases for both phases endemic ( $p < p_c$ ) and epidemic ( $p \geq p_c$ ). As found in figure 2a the cluster size at  $p_c$  strongly fluctuates and therefore, the time behavior of the number of cases also fluctuates. The variation of the number of cases with time is shown in figure 3a for three cases (just below  $p_c$ , at  $p_c$  and above  $p_c$ ) with only one initial infectious site. In both cases, the number of cases increases up to a maximum and then decrease because the number of susceptibles decreases. In the endemic phase, the number of connections between occupied sites in the cluster is mostly 1 and does not allow a significant increase of the number of cases (the behavior in this case is under estimated since all the clusters should contribute to this increase). For susceptible densities around  $p_c$  this situation persists for a long time and the number of cases increases linearly with time showing a normal diffusion of the disease. In the epidemic phase the increase becomes exponential indicating a new kind of *super-diffusion* [13, 14] of the disease, due mainly to the increasing number of connections in the cluster (as shown in figure 3b). This exponential growth is also observed for *SIR* models [15] where the rate is proportional to the basic reproduction rate  $R_0$  which corresponds in our case to the average number of connections in the cluster. We have also performed a Monte-Carlo simulation to the measles propagation in a more realistic sample (births, deaths, incubation and latent periods etc.) where the average infections is 2 for each infectious individual and found also an exponential growth of the infected cases [16]. Therefore, this exponential growth does not seem to depend on the topology of the sample but the rate is sensitive to the geometry of the network. Note in the present work that in the case of more than one initial infectious site (see figure 3c) the exponential growth behavior does not change but the growing rate fluctuates due to the fluctuating number of connections. The average rate of the exponential growth  $\gamma$  (corresponding to the characteristic time of the epidemics) is shown in

figure 4 to increases as  $Ln(p)$  above  $p_c$  while the period of this epidemic behavior decreases. From this figure we can conclude that when the characteristic time decreases below 5 (or  $\gamma$  increases above 0.2), the epidemic behavior takes place. This behavior seems to have a direct application in epidemiology since it provides a method for the estimation of the serological situation (density of susceptibles) from the characteristic time which is easily measurable. Therefore, this result stimulates a proposal for a serological examination for a given childhood disease in a sample of age school children, but during an epidemic period to compare a realistic behavior with that obtained in this paper.

Now let us examine the case of adding different infection probabilities to this system. We consider that a site  $i$  infects another site  $j$  with a probability  $p_n$  if  $j$  is a neighbor of  $i$  and  $p_{sc}$  if it is a short cut. The motivation of this investigation is that a susceptible child has a different probability to be infected by his brothers (or sisters) than by the other children meeting him at the school. We see clearly a double diffusion behavior in figure 5 (for  $p_n = 0.1$  and  $p_{sc} = 0.9$ ), where the number of infected starts growing exponentially up to the characteristic time ( $1/\gamma$ ), then it increases as a power law up to a new characteristic time from which it grows again exponentially with the same rate. The slow diffusion is due to the small contact probability for the neighbors ( $p_n = 0.1$ ) and has been observed in other fields [17]. This slow diffusion appears very short because the number of  $NN$  is very small ( $k = 2$ ). It should be interesting to investigate this double diffusion for larger  $k$  (which is the case of animal diseases).

## 5 Conclusion

We have investigated in this article the statistics of the cluster sizes in a one dimensional  $SWN$  by taking into account the  $NN$  and  $SC$  fluctuations. We found that these fluctuations decrease  $p_c$  as a power law with a small exponent leading to a new expression for the percolation threshold. We found also that cluster size fluctuations is the quantity governing the phase transition in such a network. On the other hand, in order to apply our results to the measured quantities in epidemiology, we have studied the dynamics of the disease propagation in such clusters. We

found in epidemic phases a *super-diffusive* with an exponentially growing number of infected sites, while at  $p_c$  this number increases as a power law. The growing characteristic time is larger than 5 in the endemic situation and decreases linearly with  $\ln(p)$  in the epidemic phase. This result provides a way to estimate the density of susceptibles in the epidemic phase. We propose then a serological investigation in epidemic situations to check this behavior. Finally, we examined the case where the infection probability is very small in the  $NN$  compared to the  $SC$ . The dynamical behavior of infected cases shows a double diffusion with two characteristic times, and a power-law increase (deceleration) between them. We think that this effect is useful for samples with large  $NN$  and shows a way to stop the propagation of the epidemic for other diseases.

### ACKNOWLEDGEMENTS

One of the authors (NZ) would like to thank the Arab Fund for Economic and Social Development for the financial support and the staff of the I.U.S.T.I., Université de Provence - Marseille for hospitality during the progress of this work. We thank Professor M.Barthélémy for fruitful discussions and Professor A.M.Dykhne for drawing our attention to the double diffusion behavior.

# References

- [1] B.Bollobas, *Random Graphs* (Academic Press, New York) 1985.
- [2] S.Milgram, *Psychology Today* **2** (1967) 60.
- [3] D.J.Watts, *Small Worlds* (Princeton University Press, Princeton) 1999.
- [4] D.J.Watts and S.H.Strogatz, *Nature* **393** (1998) 440.
- [5] M.E.J. Newman and D.J.Watts, *Phys.Lett.A* **263** (1999) 341.
- [6] M.E.Newman, *J.Stat.Phys.* **101**, 819 (2000).
- [7] M.E.Newman et D.J.Watts, *Phys.Rev.E* **60** (1999) 7332.
- [8] D.Stauffer and A.Aharony, *Percolation theory*, 2nd Ed. (Taylor and Francis, London) 1994;  
D.J.Bergman and D.Stroud, *Solid State Phys.* **46**, 147 (1992).
- [9] R.Pastor-Satorras et A.Vespignani, *Phys.Rev.E*, **63**, 066117 (2001).
- [10] C.Moore and M.E.J.Newman, *Phys.Rev.E* **61**, 5678 (2000); *idem* **62**, 7059 (2000).
- [11] M.Kuperman and G.Abramson, *Phys.Rev.Lett.* **86**, 2909 (2001).
- [12] C.Castellano, M..Marsili et A.Vespignani, *Phys.Rev.Lett.* **85** (2000) 3536.
- [13] P.Lévy, *Théory de l'addition des variables aléatoire* (Gautier-Villars, Paris, 1937;  
M.Shlesinger, G.M.Zaslavsky and U.Frish *Lévy flights and related topics in Physics* (Springer,  
Berlin) 1995; J.P.Bouchaud and A.Georges, *Phys.Rep.* **195**, 12 (1990).
- [14] S.N. Evangelou and D.E.Katsanos, *Phys.Lett.A* **164**, 456 (1992).
- [15] R.M.Anderson and R.M.May, *Infectious diseases of humans. Dynamics and control*, (Oxford  
University Press, Oxford) 1991.
- [16] N.Zekri and J.P.Clerc, unpublished.
- [17] A.M.Dykhne, private communication.

## Figure Captions

**Figure 1**     **a)** Cluster size (number of sites in the cluster) versus concentration of the occupied sites for three cases:  $\phi = 6$  (solid curve);  $\phi = 30$  (dotted curve) and  $\phi = 30$  with fluctuations  $\delta k = 2$ ,  $\delta\phi = 15$  (dashed-dotted curve).

**b)**  $p_c$  versus  $\delta\phi$  (sites) for  $\phi = 30$  sites. The solid line is a fit of the data.

**Figure 2**     **a)** Cluster size fluctuations (sites) versus the occupied sites concentration ( $\phi = 6$  sites). The solid curve is a guide for the eyes.

**b)** Distribution of the cluster size (sites) for fixed ( $k = 2$ ,  $\phi = 6$ ) in a semi-log plot at  $p_c$  (solid curve) and  $p = 1\%$  (dotted curve). The dotted line is a linear fit of the data below  $p_c$ . The insert is a log-log plot of the distribution at  $p_c$  with a linear fit.

**c)** Variation of the exponent  $x$  with the number of short cuts  $\phi$  (sites). The solid line is a linear fit of the data to  $5.6 \cdot 10^{-3}$ .

**Figure 3**     **a)** Number of cases versus time for three different cases;  $p = 3.5\%$  (solid curve),  $p = 4.5\%$  (dashed curve) and  $p = 8\%$  (dotted curve). Insert: log-log plot with a power law fit of  $p = 4.5\%$  and an exponential fit of  $p = 8\%$ .

**b)** Distribution of the number of connections (acquaintances) in the largest cluster for  $p = 3.5\%$  (solid curve),  $p = 5\%$  (dashed curve) and  $p = 10\%$  (dotted curve).

**c)** The rate of the exponential growth (in arbitrary units) versus number of initial infectious sites. The horizontal line is the average rate.

**Figure 4**     The rate of the exponential growth versus  $p$ . The solid line is a fit of the curve linearly with  $\ln(p)$ .

**Figure 5**     The Number of infected cases versus time (in arbitrary units) for one initial infectious site and an infection probability one (solid curve), and the probabilities of infection:

$p_n = 0.1$  and  $p_{sc} = 0.9$  (dotted curve). The dashed curve is a power law fit of the second data in the region of the double diffusion.

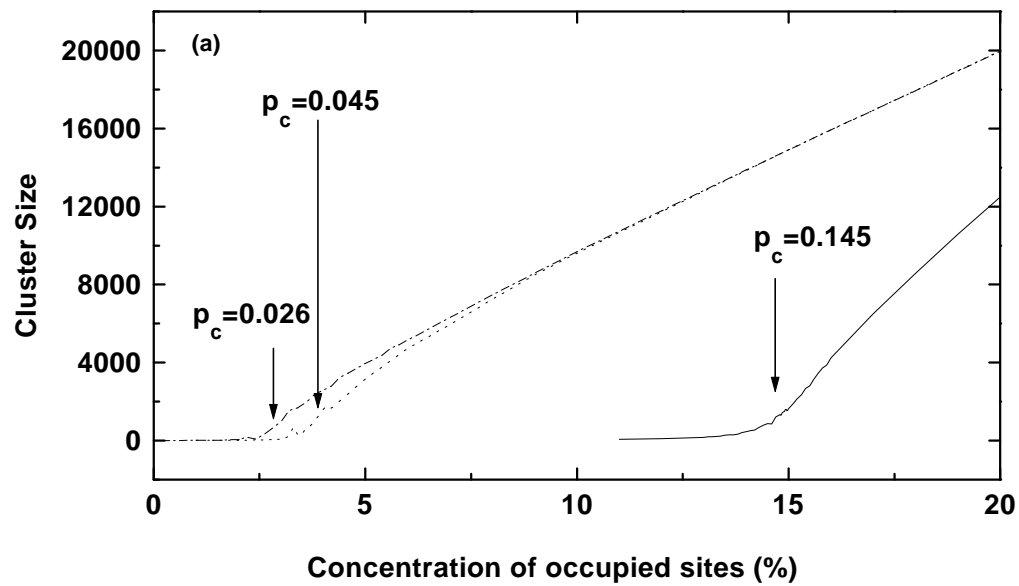


FIGURE 1

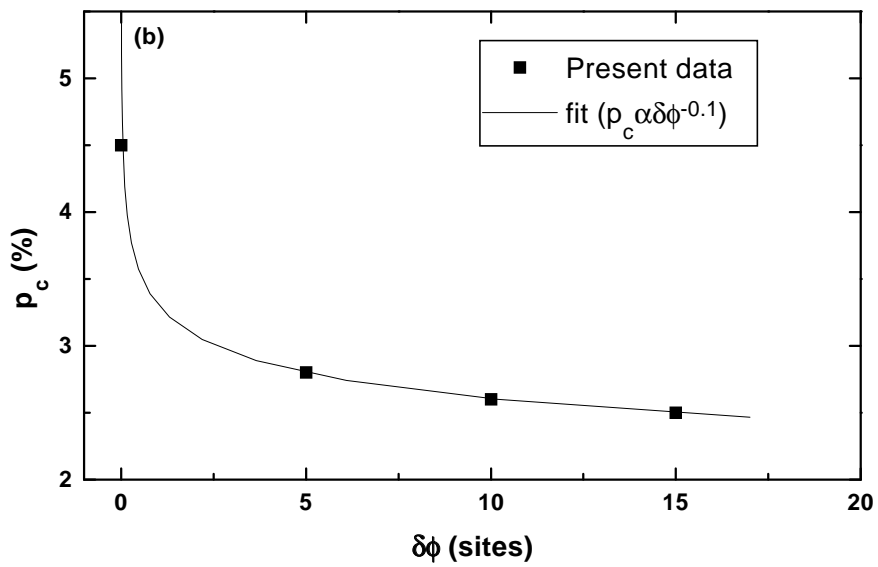
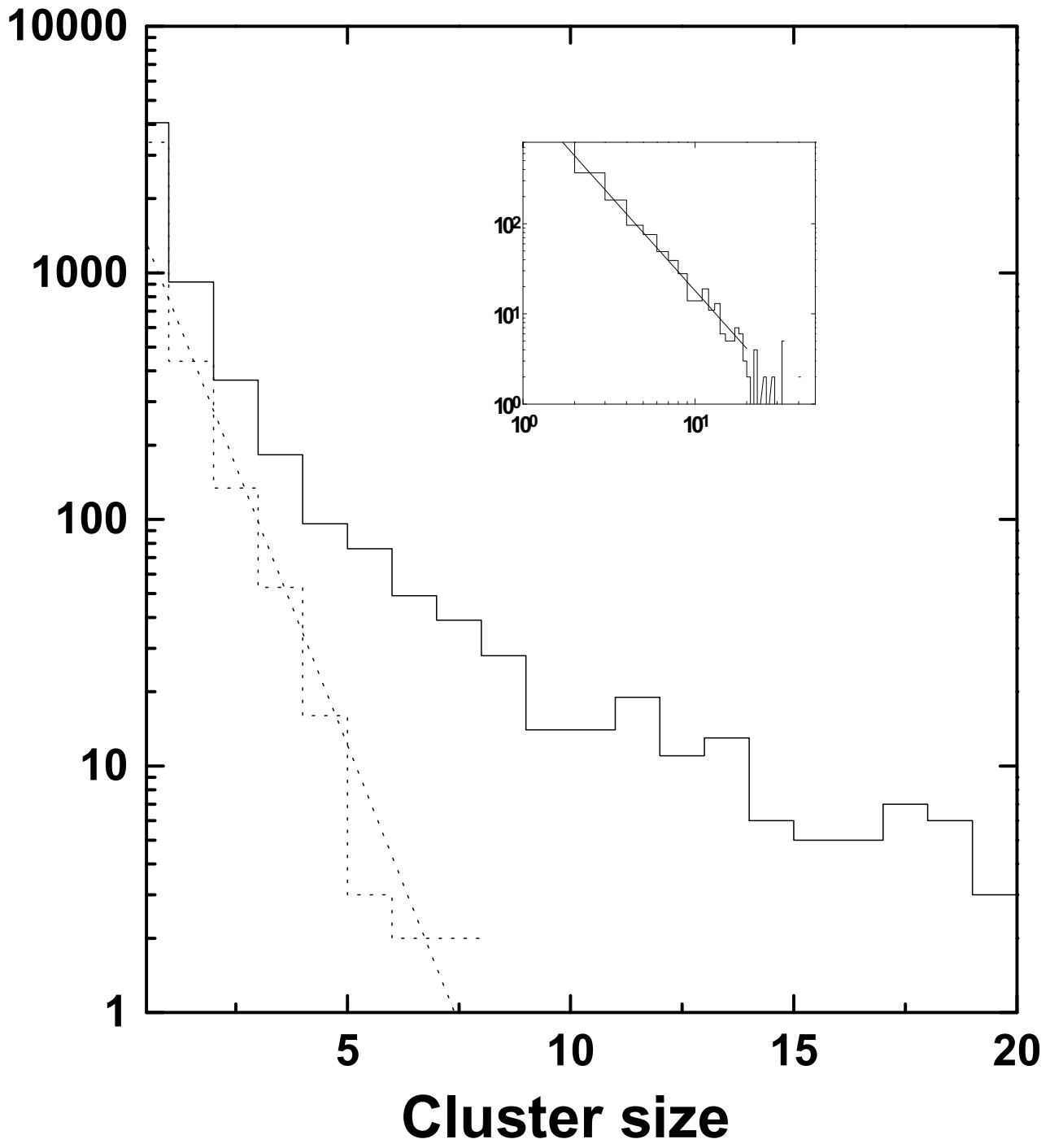


FIGURE 1



**FIGURE 2b**

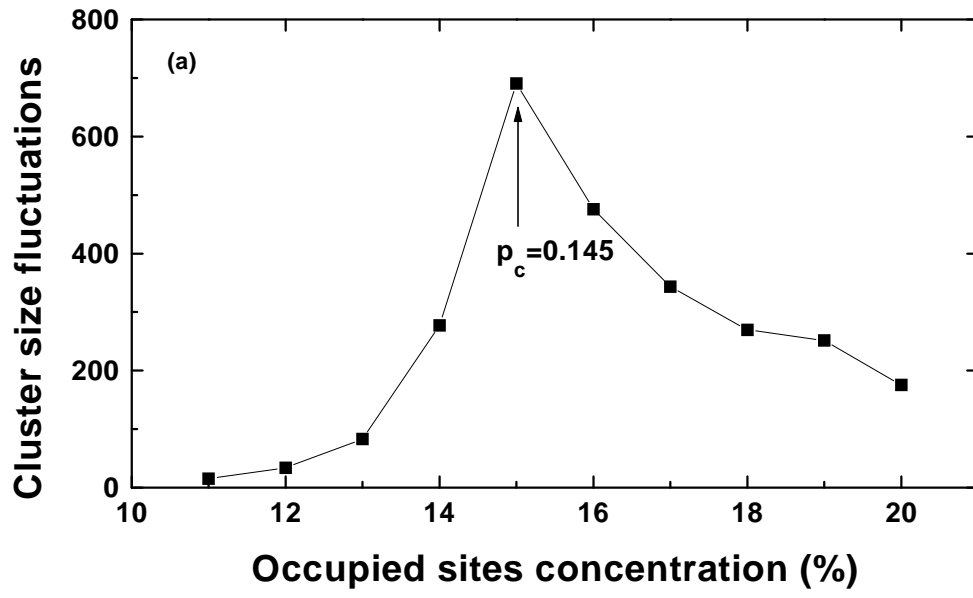
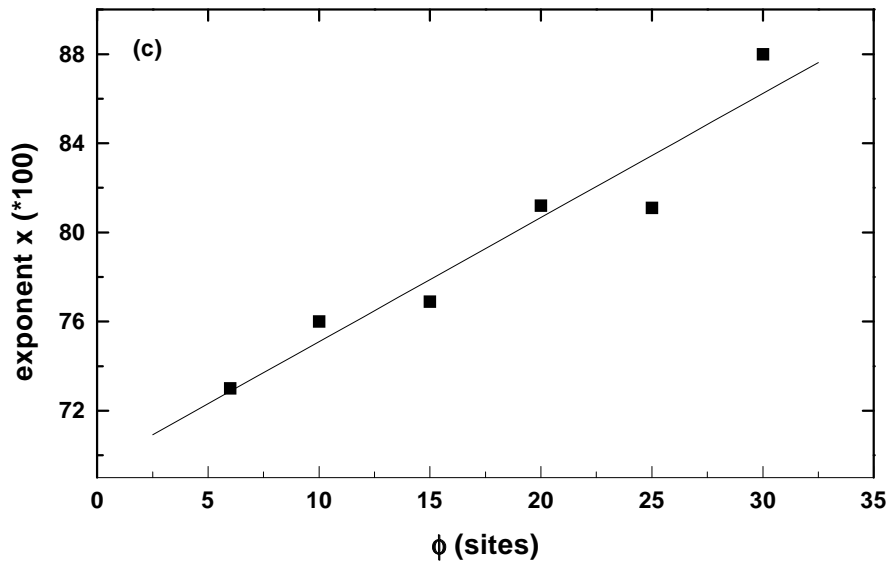
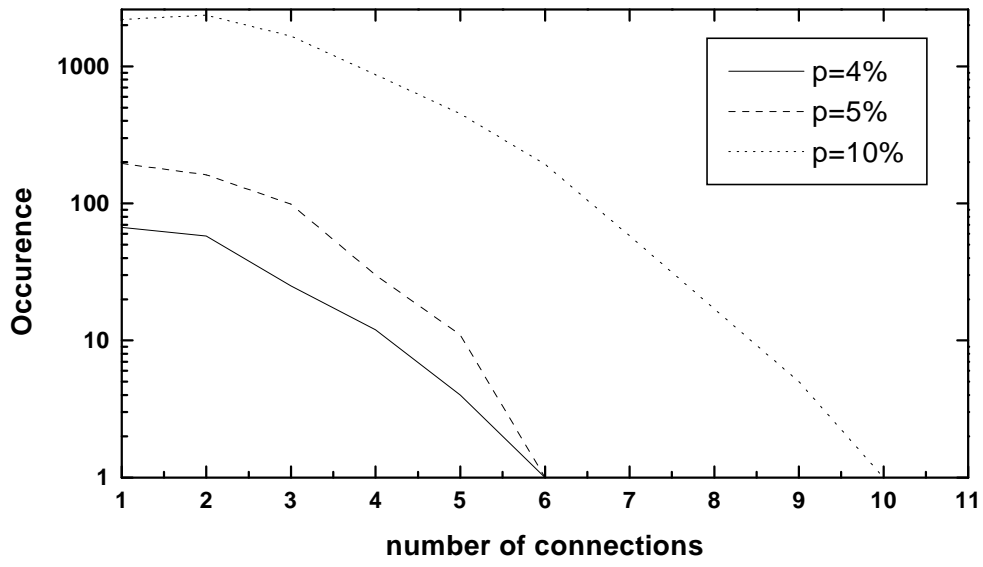


FIGURE 2



**FIGURE 2**



**FIGURE 3b**

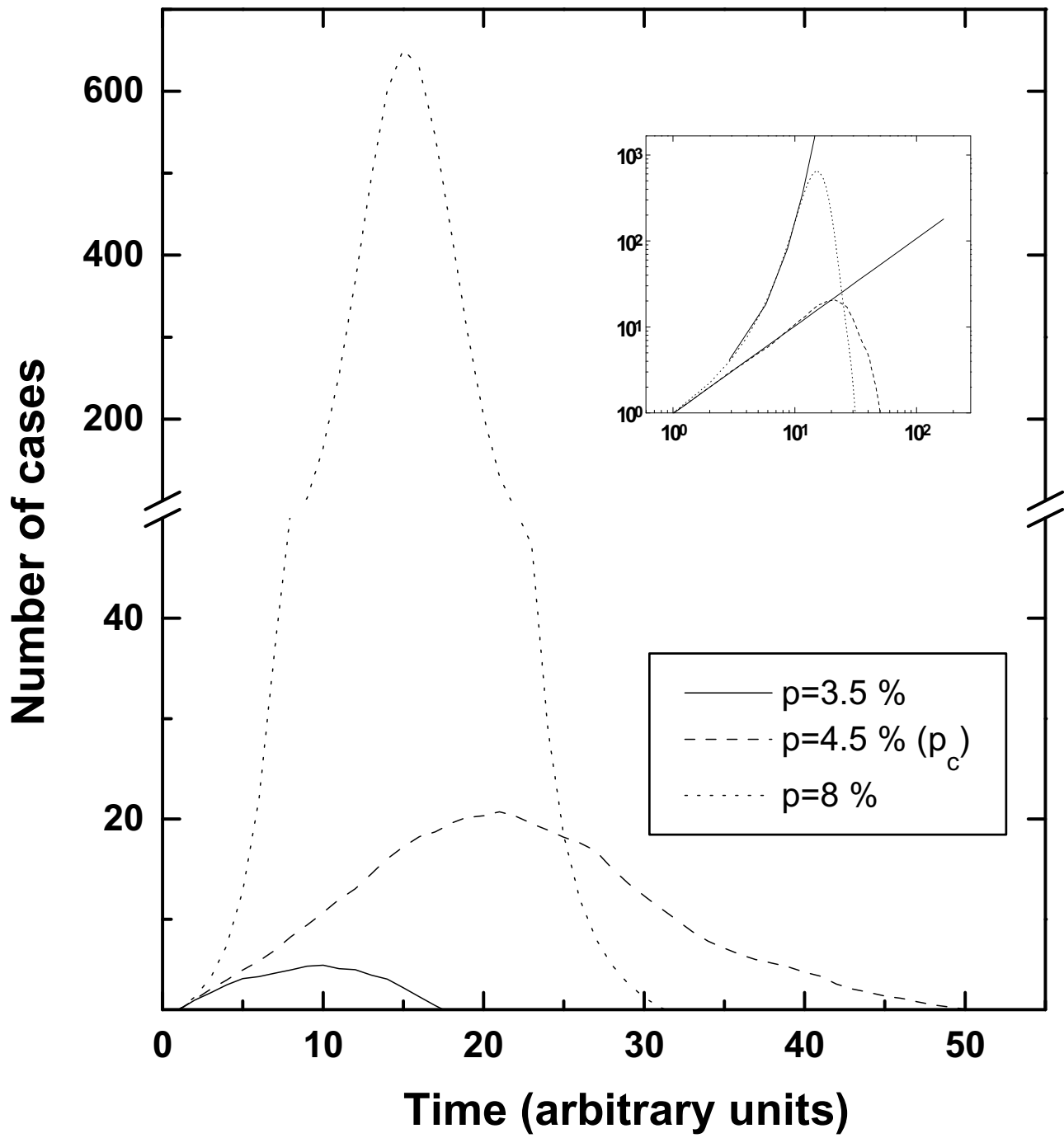


**FIGURE 3a**

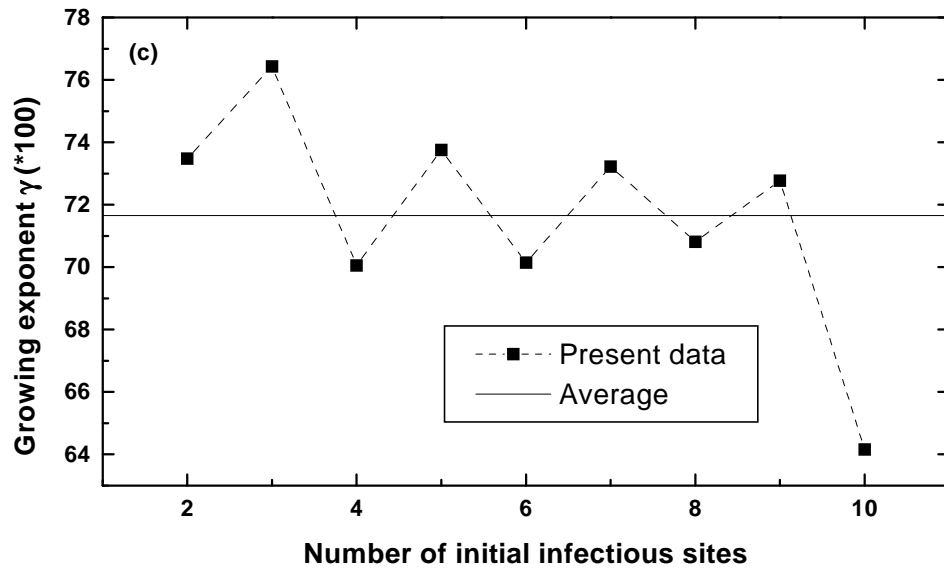


**FIGURE 3**

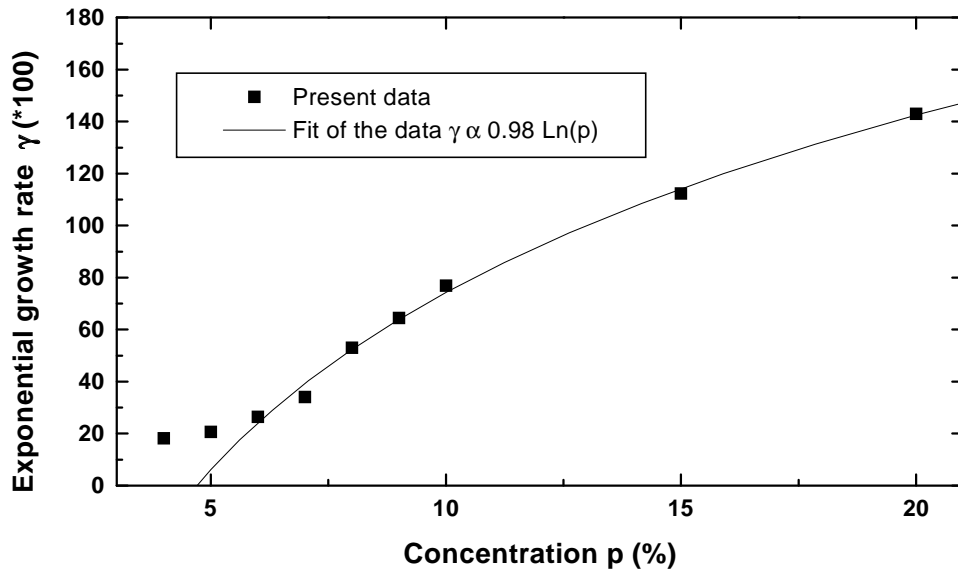


**FIGURE 4**

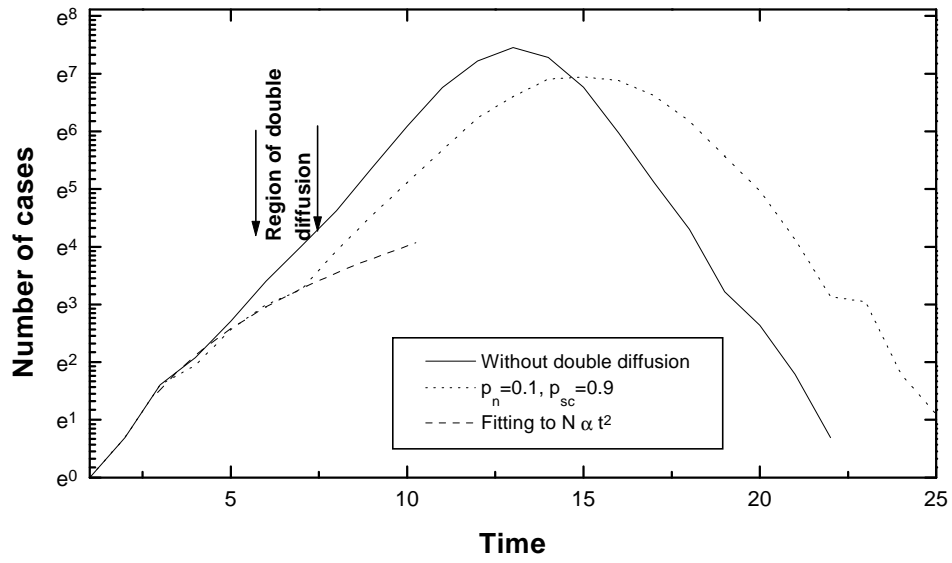


**FIGURE 5**